



This is a repository copy of *Large-baseline quantum telescopes assisted by partially distinguishable photons*.

White Rose Research Online URL for this paper:

<https://eprints.whiterose.ac.uk/225582/>

Version: Published Version

Article:

Modak, S. and Kok, P. orcid.org/0000-0002-6608-330X (2025) Large-baseline quantum telescopes assisted by partially distinguishable photons. *Physical Review A*, 111 (4). 043701. ISSN 2469-9926

<https://doi.org/10.1103/physreva.111.043701>

Reuse

This article is distributed under the terms of the Creative Commons Attribution (CC BY) licence. This licence allows you to distribute, remix, tweak, and build upon the work, even commercially, as long as you credit the authors for the original work. More information and the full terms of the licence here:

<https://creativecommons.org/licenses/>

Takedown

If you consider content in White Rose Research Online to be in breach of UK law, please notify us by emailing eprints@whiterose.ac.uk including the URL of the record and the reason for the withdrawal request.



eprints@whiterose.ac.uk
<https://eprints.whiterose.ac.uk/>

Large-baseline quantum telescopes assisted by partially distinguishable photons

Subhrajit Modak and Pieter Kok 

Department of Physics & Astronomy, The University of Sheffield, Hounsfield Road, Sheffield S3 7RH, United Kingdom

 (Received 15 January 2025; accepted 17 March 2025; published 1 April 2025)

Quantum entanglement can be used to extend the baseline of telescope arrays in order to increase the spatial resolution. In one proposal by Marchese and Kok [*Phys. Rev. Lett.* **130**, 160801 (2023)], identical single photons are shared between receivers and interfere with a star photon. In this paper we consider two outstanding questions: (i) what is the precise effect of the low photon occupancy of the mode associated with the starlight? and (ii) what is the effect on the achievable resolution of imperfect indistinguishability (or partial distinguishability) between the ground and star photons? We find that the effect of distinguishability is relatively mild, but low photon occupancy of the optical mode of the starlight quickly deteriorates the sensitivity of the telescope for higher auxiliary photon numbers.

DOI: [10.1103/PhysRevA.111.043701](https://doi.org/10.1103/PhysRevA.111.043701)

I. INTRODUCTION

Large baseline imaging is a well-known technique for improving the resolution of telescopes [1–4]. It has recently been used to resolve the spatial features of a black hole in the radio-frequency spectrum [5], with a baseline comparable to the diameter of the earth. This was possible because antennas can track both the amplitude and the phase of radio-frequency waves and reconstruct the wave propagation characteristics. In contrast, at optical frequencies the amplitude and phase information must be retrieved via interferometry, which severely limits the baseline of optical telescopes. Light collected in the telescopes must travel through light pipes or optical fibers, which practically limits the baseline due to construction constraints or photon losses, respectively.

Quantum technologies can be used to improve the performance of telescopes by choosing the optimal quantum observable [6–12] or extending the baseline using quantum repeater protocols [13] and quantum error correction [14]. Recently, Marchese and Kok proposed a repeaterless method to extend the baseline of a telescope by employing multiple single-photon sources at the ground level that interfere at the receiver sites with photons originating from astronomical objects [15] (see Fig. 1). This minimizes the distance traveled by the photons that carry information about the astronomical objects and allows for redundancy in the ground-based photons to combat transmission losses over large distances. In this paper we address two outstanding open questions that arose from Ref. [15]: (i) what is the precise effect of the low photon occupancy of the mode associated with the starlight? and (ii) what is the effect on the achievable resolution of imperfect

indistinguishability (or partial distinguishability) between the ground and star photons.

This paper is organized as follows. In Sec. II, we recall the technical details of the repeaterless quantum telescope of Ref. [15], and in Sec. III, we provide the analysis of partially distinguishable photons. In Sec. IV, we establish the achievable resolution for the telescope, taking into account single-mode photon occupancy. We conclude in Sec. V.

II. THE QUANTUM TELESCOPE PROTOCOL

We assume that a pointlike astronomical object, such as a distant star, is sufficiently far away that the incoming light can be effectively approximated by a plane wave. A photon from this object will arrive in two receivers of the telescope, *A* and *B*, separated by a distance *L*, in the superposition state

$$|\psi_{\text{in}}\rangle = \frac{|1\rangle_A |0\rangle_B + e^{i\phi} |0\rangle_A |1\rangle_B}{\sqrt{2}}, \quad (1)$$

where $\phi = kl = kL \sin \theta$ is the phase difference between the two receivers due to the path difference *l* that originates from the direction θ of the incoming wave with wave number *k* (see Fig. 1). The star photon is collected by the receivers *A* and *B*, and interferes locally at the receivers with *N* ground-based photons in interferometers *U*. The ground-based sources *s_n* each emit a photon $|s_n\rangle$ in a superposition of two modes, *a_n* and *b_n*, that propagate towards receivers *A* and *B*, respectively:

$$|s_n\rangle = \frac{|1\rangle_{a_n} |0\rangle_{b_n} + |0\rangle_{a_n} |1\rangle_{b_n}}{\sqrt{2}}. \quad (2)$$

This state is easily achieved with a 50:50 beam splitter placed behind the single-photon source. The two-mode state $|s_n\rangle$ is entangled in the photon number degree of freedom, since in field theory, photons are excitations of the field modes and it is the optical modes that constitute the entangled systems. To avoid confusion with qubit entanglement, we refer to this as “mode-entangled” states. For the original debate on this distinction, see Refs. [16–19].

Published by the American Physical Society under the terms of the Creative Commons Attribution 4.0 International license. Further distribution of this work must maintain attribution to the author(s) and the published article’s title, journal citation, and DOI.

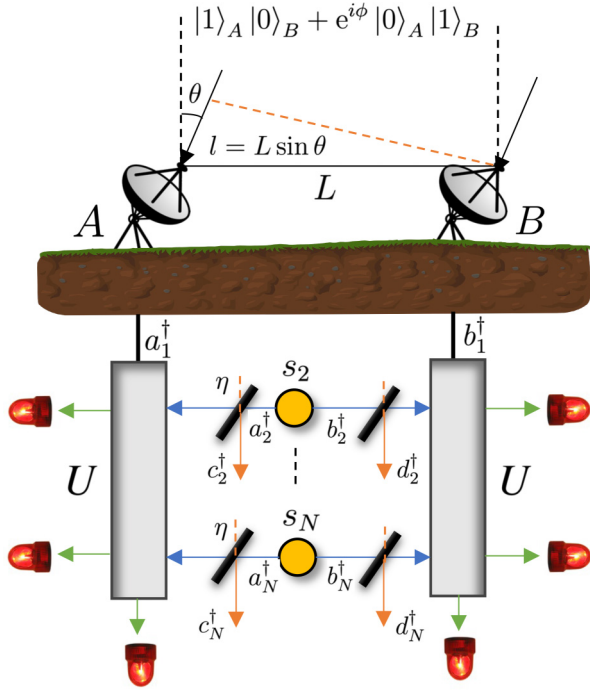


FIG. 1. The proposal of Ref. [15]: two receivers, A and B, separated by a distance L , receive photons from a pointlike astronomical object and from sources S_2, \dots, S_N located midway between the receivers. The path length of the star photon is kept short by collocating the interferometers U with the receivers. The photons sent from sources S_2 to S_N experience reduced transmission $\eta^2 \leq 1$ due to fiber losses. The measurement statistics are used to estimate the declination angle θ , encoding the position of the star.

The creation and annihilation operators of the ground-based modes are $\{a_n^\dagger, a_n\}$ and $\{b_n^\dagger, b_n\}$, and the input state becomes

$$|\psi\rangle_{\text{tot}}^{\text{in}} = \left(\frac{1}{2}\right)^{\frac{N}{2}} \prod_{n=1}^N (a_n^\dagger + e^{i\phi\delta_{n,1}} b_n^\dagger) |0\rangle, \quad (3)$$

where the Kronecker delta ensures that the phase shift ϕ is applied to mode 1, the starlight mode. Here $|0\rangle$ is the vacuum state. The interferometers U implement a discrete quantum Fourier transform (QFT), and detecting $D \leq N$ photons allows one to reconstruct the probability distributions $P_{\mathbf{d}}(\phi)$ in the presence of losses, where \mathbf{d} indicates the detector signature. Reference [15] showed that this distribution contains a significant amount of information about the phase ϕ and therefore the angular position of the star θ . We assume perfect number-resolving detectors.

The Fisher information, which measures the information about ϕ in the probability distribution, is given by [15]

$$F_N(\phi) = \sum_{\mathbf{d}} \sigma_N P_{\mathbf{d}}(\phi) \left(\frac{\partial \ln P_{\mathbf{d}}(\phi)}{\partial \phi} \right)^2, \quad (4)$$

where σ_N is the total number of possible detector outcomes. Including transmission losses for the ground photons, the

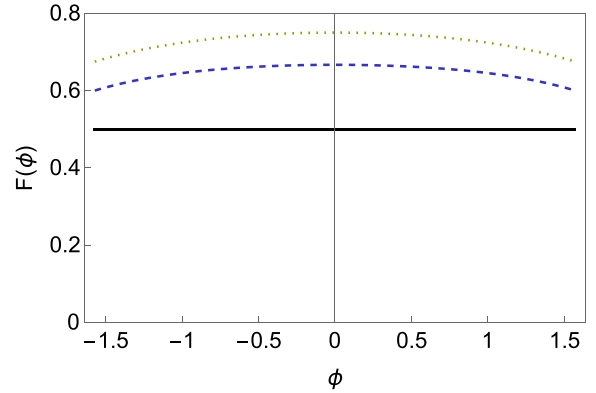


FIG. 2. The dependence of the Fisher information on ϕ for various numbers N of photons in the setup under the ideal condition of no loss (solid black line, $N = 2$; dashed blue line, $N = 3$; and dotted line, $N = 4$). The Fisher information increases with the photon number as $F_N(\phi) = 1 - 1/N$.

Fisher information reduces to

$$F_N^{\text{loss}} = \sum_{k=0}^{N-1} p^k (1-p)^{N-1-k} \binom{N-1}{k} F'_{N-k}, \quad (5)$$

where F'_{N-k} is the Fisher information for $D = N - k$ detected photons, k is the number of photons lost, and p is the probability of a single-photon loss. We assume that the loss on the star photon is negligible and that the dominant loss is from the fiber transmission losses over long distances. In the case of no loss ($p = 0$), the Fisher information still depends on ϕ , as shown in Fig. 2 for $N \geq 3$. Hence, the optimal arrangement is to include a variable phase shift in one receiver that balances the interferometer in such a way that the receivers “point” to the source, i.e., $\phi \sim 0$.

III. DISTINGUISHABILITY OF PHOTONS

Next, we consider how the distinguishability between photons affects the Fisher information. We take the star photon as the reference photon and study how imperfect mode-matching of the ground-based photons to the star photon affects the resolution. Our approach is as follows: the spatiotemporal characteristics of the star photon are labeled with index μ . A ground-based photon in a single mode a_j with a slightly different spatiotemporal character can then be described by a mode that is a superposition of mode a^μ and an orthogonal mode a_j^ν . These modes have corresponding mode operators that satisfy the usual bosonic commutation relations: $[\hat{a}^\mu, \hat{a}^{\dagger\nu}] = [\hat{b}^\mu, \hat{b}^{\dagger\nu}] = \delta_{\mu\nu}$ and $[\hat{a}^\mu, \hat{a}^\nu] = [\hat{b}^\mu, \hat{b}^\nu] = 0$. There are two possibilities: all the ground-based photons may be different from the star photon but identical to each other or all the ground-based photons are also slightly distinguishable from each other. In the latter case, the part of the mode for photon j that is orthogonal to the star photon mode must also be orthogonal to the other ground-based photons, and we require an extra index j on the orthogonal mode: $a^\nu \rightarrow a_j^\nu$. We model the distinguishability between the photons using the

parameter $\mathcal{I} \in [0, 1]$:

$$\begin{aligned} \hat{a}_1 &= \hat{a}_1^\mu, \\ \hat{a}_j &= \sqrt{\mathcal{I}} \hat{a}_j^\mu + \sqrt{1 - \mathcal{I}} \hat{a}_j^{\nu_j}, \\ \hat{b}_1 &= \hat{b}_1^\mu, \\ \hat{b}_j &= \sqrt{\mathcal{I}} \hat{b}_j^\mu + \sqrt{1 - \mathcal{I}} \hat{b}_j^{\nu_j}. \end{aligned} \quad (6)$$

In this work, we focus on the problem of phase estimation with multiple ground-based photons, where the degree of indistinguishability \mathcal{I} is assumed to be known and uniform across the photons.

The initial state of the incoming star photon and the ground-based photons is given by

$$|\psi\rangle_{\text{tot}}^{\text{in}} = \frac{1}{\sqrt{2}}(a_1^\dagger + e^{i\phi} b_1^\dagger) \otimes \prod_{j=2}^N \frac{a_j^\dagger + b_j^\dagger}{\sqrt{2}} |0\rangle. \quad (7)$$

Following the transformation in Eq. (6), the distinguishability between photons is then modeled by

$$\begin{aligned} a_j^\dagger &= \sqrt{\mathcal{I}} a_j^{\dagger\mu} + \sqrt{1 - \mathcal{I}} a_j^{\dagger\nu_j}, \\ b_j^\dagger &= \sqrt{\mathcal{I}} b_j^{\dagger\mu} + \sqrt{1 - \mathcal{I}} b_j^{\dagger\nu_j}, \end{aligned} \quad (8)$$

where $j \in [2, N]$ accounts for only the ground-based photon sources.

As in Ref. [15], we analyze the photon loss of ground-based fiber transmission using the well-known beam-splitter model where the transmissivity η is determined by the fiber loss $\eta = e^{-L/4L_0}$, where each photon travels over a length $L/2$, and L_0 is the attenuation length of the fiber. For simplicity, we assume that L_0 is the same for all fibers. The transformed mode operators for the ground-based photons are thus written as

$$\begin{aligned} a_j^{\dagger\kappa} &= \eta a_j^{\dagger\kappa} + \sqrt{1 - \eta^2} c_j^{\dagger\kappa}, \\ b_j^{\dagger\kappa} &= \eta b_j^{\dagger\kappa} + \sqrt{1 - \eta^2} d_j^{\dagger\kappa}, \end{aligned} \quad (9)$$

where $\kappa \in \{\mu, \nu_j\}$ indicates the mode of the ground-based photons and $\{c_j^\dagger, c_j\}$ ($\{d_j^\dagger, d_j\}$) are the vacuum field operators on either side of the installation.

At each site, the ground-based photon modes are mixed with the star photon modes. This is done by implementing QFT to the set of input photonic modes. This transformation appears as a simple balanced beam-splitter in the case with two photons, generating the following outputs for the modes on the left:

$$\begin{aligned} a_{1,\text{out}}^{\dagger\kappa} &= \frac{1}{\sqrt{2}}(-a_{1,\text{in}}^{\dagger\kappa} + a_{2,\text{in}}^{\dagger\kappa}), \\ a_{2,\text{out}}^{\dagger\kappa} &= \frac{1}{\sqrt{2}}(a_{1,\text{in}}^{\dagger\kappa} + a_{2,\text{in}}^{\dagger\kappa}), \end{aligned} \quad (10)$$

and analogously for the b_i modes on the right. Therefore, for $N = 2$ the overall initial state in Eq. (7) becomes

$$\begin{aligned} |\psi\rangle_{\text{tot}}^{\text{out}} &= \frac{1}{2} \left(\frac{(-a_1^{\dagger\mu} + a_2^{\dagger\mu})}{\sqrt{2}} + e^{i\phi} \frac{(-b_1^{\dagger\mu} + b_2^{\dagger\mu})}{\sqrt{2}} \right) \\ &\otimes \left[\alpha \left(\eta \frac{(a_1^{\dagger\mu} + a_2^{\dagger\mu})}{\sqrt{2}} + \sqrt{1 - \eta^2} c_2^{\dagger\mu} \right) \right. \end{aligned}$$

$$\begin{aligned} &+ \beta \left(\eta \frac{(a_1^{\dagger\nu} + a_2^{\dagger\nu})}{\sqrt{2}} + \sqrt{1 - \eta^2} c_2^{\dagger\nu} \right) \\ &+ \alpha \left(\eta \frac{(b_1^{\dagger\mu} + b_2^{\dagger\mu})}{\sqrt{2}} + \sqrt{1 - \eta^2} d_2^{\dagger\mu} \right) \\ &\left. + \beta \left(\eta \frac{(b_1^{\dagger\nu} + b_2^{\dagger\nu})}{\sqrt{2}} + \sqrt{1 - \eta^2} d_2^{\dagger\nu} \right) \right] |0\rangle, \quad (11) \end{aligned}$$

where $\alpha = \sqrt{\mathcal{I}}$ and $\beta = \sqrt{1 - \mathcal{I}}$ are the amplitudes corresponding to the relative indistinguishability and the opposite, respectively. For $N = 2$, we do not need to disambiguate ν with an index 2.

To find the Fisher information, we must calculate the probabilities

$$P_{\mathbf{d}}(\phi) = |\langle \mathbf{d} | \psi \rangle_{\text{tot}}^{\text{out}}|^2, \quad (12)$$

for the detector signatures $|\mathbf{d}\rangle = |\mathbf{d}^\mu, \mathbf{d}^\nu\rangle$, where $|\mathbf{d}\rangle = |d_1, d_2, d_3, d_4\rangle$ and $d_i \in \{1, 2\}$ is the number of photons found in detector i . Evidently, two photons can be distributed among various modes and detectors in a number of ways. The relative phase shift will turn to a global phase when both the photons are picked up by the same detector or by separate detectors on the same side. Therefore, we can only obtain information about ϕ when two photons are detected in the same mode and on different sides of the detectors. Only the following configurations give rise to probabilities that contribute to the Fisher information:

$$\begin{aligned} P_{|a_2^{\dagger\mu}, b_1^{\dagger\mu}\rangle}(\phi) &= P_{|a_1^{\dagger\mu}, b_2^{\dagger\mu}\rangle}(\phi) = \frac{\eta^2 \mathcal{I}}{8} (1 - \cos \phi), \\ P_{|a_1^{\dagger\mu}, b_1^{\dagger\mu}\rangle}(\phi) &= P_{|a_2^{\dagger\mu}, b_2^{\dagger\mu}\rangle}(\phi) = \frac{\eta^2 \mathcal{I}}{8} (1 + \cos \phi). \end{aligned} \quad (13)$$

We point out that no information about the correlation is available with only one observed photon. Hence F_1' is always 0 and the total Fisher information is

$$F_2^{\text{loss}}(\phi) = \frac{1}{2}(1 - p)\mathcal{I}, \quad (14)$$

where $p = 1 - \eta^2$ is the probability of losing a single photon.

The situation gets quite different when an extra ground-based photon is added. We further emphasize that each photon at the ground base is identifiable from the reference to different degrees. Upon considering all the detection events, the Fisher information yields

$$\begin{aligned} F_3^{\text{loss}}(\phi) &= \frac{1}{2}(1 - p)^2 \frac{6(1 + \cos \phi)}{5 + 4 \cos \phi} \mathcal{I}_2 \mathcal{I}_3 \\ &+ \frac{1}{2}(1 - p)^2 [(\mathcal{I}_2 + \mathcal{I}_3) - 2\mathcal{I}_2 \mathcal{I}_3] \\ &+ \frac{1}{2}p(1 - p)(\mathcal{I}_2 + \mathcal{I}_3), \end{aligned} \quad (15)$$

where \mathcal{I}_j measures the degree of indistinguishability for j th ground-based photons. The Fisher information in Eq. (15) consists of terms that arise when all the photons are detected and a single photon is lost. Events with two photon losses are not relevant, since they do not contribute to the Fisher information of the $N = 3$ case. As the number of ground-based photons increases, it is expected to contribute more to the

Fisher information. However, the relative distinguishability of photons appears to limit this advantage. An improvement over this can still be made if the photons are kept identical, i.e., $\mathcal{I}_2 = \mathcal{I}_3$. Next, we examine the extent to which the number of ground-based photons can be increased.

IV. ACHIEVABLE RESOLUTION

Next, we consider the case of a weak thermal source at optical frequencies. The rate of photon emission ε within each coherence time interval is considerably less than 1 [20]. Therefore, the density operator for the optical field in each interval becomes, to a good approximation,

$$\rho = (1 - \varepsilon)\rho_0 + \varepsilon\rho_1, \quad (16)$$

where ρ_1 is the one-photon state and $\rho_0 = |0\rangle\langle 0|$ is the zero-photon state. Two-photon events are considered insignificant for the remainder of the discussion. The total probability of detecting d photons in the N -photon setup becomes

$$P_T(\mathbf{d}) = (1 - \varepsilon)P_A(\mathbf{d}) + \varepsilon P_B(\mathbf{d}), \quad (17)$$

where $P_A(\mathbf{d})$ and $P_B(\mathbf{d})$ are the probabilities for the absence and the presence of the star photon, respectively. Clearly, we cannot identify from the detection of $d < N$ photons whether a star photon is present. In this case, the Fisher information becomes

$$F(\phi) = \sum_{\mathbf{d}} \frac{\varepsilon^2}{(1 - \varepsilon)P_A(\mathbf{d}) + \varepsilon P_B(\mathbf{d})} \left(\frac{\partial P_B(\mathbf{d})}{\partial \phi} \right)^2, \quad (18)$$

where $P_A(\mathbf{d})$ does not depend on ϕ because the absence of a star photon carries no information about ϕ .

We calculate the Fisher information for various values of N . For $N = 2$, the factor ε modifies the total Fisher information:

$$F_2(\phi) = \frac{1}{2}\varepsilon(1 - p)\mathcal{I}. \quad (19)$$

Linear scaling in ε reflects the reduced rate of gaining information about ϕ . For $N = 3$, the scaling in ε remains linear when all the photons are detected. However, the situation changes when a single photon is lost (see the Appendix). This implies a deteriorated estimation due to the uncertain arrival of the star photon. Upon considering all the events, the total Fisher information results in

$$\begin{aligned} F_3(\phi) &= \frac{\varepsilon}{2}(1 - p)^2 \frac{6(1 + \cos \phi)}{5 + 4 \cos \phi} \mathcal{I}_2 \mathcal{I}_3 \\ &+ \frac{\varepsilon}{2}(1 - p)^2 [(\mathcal{I}_2 + \mathcal{I}_3) - 2\mathcal{I}_2 \mathcal{I}_3] + \sum_i \mathcal{F}_2^i, \end{aligned} \quad (20)$$

where \mathcal{F}_2^i records various contributions when a single photon is lost, and i runs over all such possible configurations (see the Appendix). In the limiting case, $\varepsilon \rightarrow 1$ and $p \rightarrow 0$, the typical scaling with N is reproduced by the Fisher information as $F_N \propto 1 - 1/N$.

Next, we look at the situation using four photons. We record an additional contribution to the Fisher information due to the higher number of photons. In order to make the expression analytically accessible, we assume all the photons are indistinguishable, while the case with distinct photons is

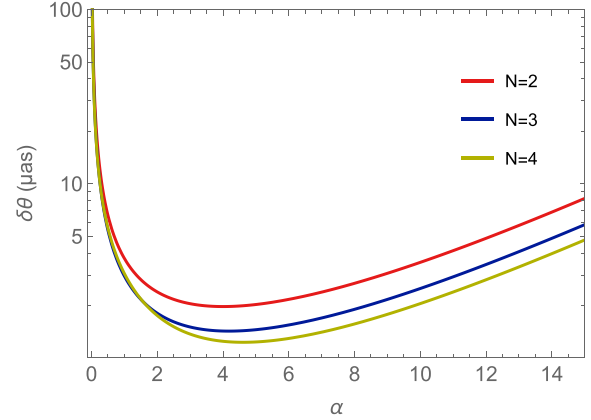


FIG. 3. The resolution angle $\delta\theta$ for identical photons at a given optical wavelength $\lambda = 628$ nm and over a typical attenuation length $L_0 = 10$ km. In an ideal situation, we consider the star photon to arrive with certainty, i.e., $\varepsilon = 1$. The resolution angle decreases at short distances and approaches a minimum as the baseline increases. Further increases in the baseline result in reduced resolution due to the predominant losses across the transmission channel. Thus, with more ground-based photons, we achieve better resolution and a shift in the minimum is observed towards larger distances, allowing for an extension of the baseline.

calculated numerically. This leads to

$$F_4(\phi) = 3\varepsilon(1 - p)^3 \frac{(9 + 7 \cos \phi)}{8(5 + 3 \cos \phi)} + \sum_i \mathcal{F}_3^i + \sum_j \mathcal{F}_2^j, \quad (21)$$

where \mathcal{F}_3^i records all the instances when a single photon is lost and \mathcal{F}_2^j does the same when two photons are lost (see the Appendix).

The achievable resolution of the telescope is captured by the statistical error $\delta\theta$ in the angle $\theta = \phi/kL$, where we used the small-angle approximation, since we are operating the telescope in the optimal regime where $\phi \approx 0$. From the error propagation formula, we have

$$(\delta\theta)^2 = \frac{(\delta\phi)^2}{k^2 L^2}, \quad (22)$$

and $(\delta\phi)^2$ is lower bounded by the Fisher information via the Cramér-Rao bound. The best resolution is, therefore, given by

$$(\delta\theta)^2 = \left(\frac{1}{kL} \right)^2 \frac{1}{F_N(\phi)}. \quad (23)$$

As expected, an increase in Fisher information leads to a better resolution.

The resolution for identical photons and $\varepsilon = 1$ is shown in Fig. 3 as a reference. In our model $\varepsilon = 1$ describes the single-photon state, which is no longer a thermal state. We include this to gain insight into how the occupation number affects the sensitivity of the imaging method. Including low photon occupancy and ground-based photons that are 96% identical to the star photon—and identical to each other—leads to the resolutions shown in Table I, where we optimized the distance L_{opt} between the receivers. The last column includes $\alpha_{\text{opt}} = L_{\text{opt}}/L_0$. The values for $\delta\theta_{\text{min}}$ are calculated for $L_0 = 10$ km

TABLE I. The table shows the parameters obtained with different N for a given emission rate of the star photon. The ground-based photons are considered to be nearly identical (96%) to the star photon, and identical to each other. The third column shows the minimum resolution $\delta\theta_{\min}$ at the optimal α_{opt} , keeping the relative phase shift ϕ fixed close to 0.

| ε | N | $\delta\theta_{\min}$ (μas) | α_{opt} |
|---------------|-----|--|-----------------------|
| 1 | 2 | 1.9797 | 4 |
| | 3 | 1.4311 | 4.1797 |
| | 4 | 1.2347 | 4.61273 |
| 0.99 | 2 | 2.0303 | 4 |
| | 3 | 1.4698 | 4.19205 |
| | 4 | 1.6888 | 4.28221 |
| 0.5 | 2 | 2.8569 | 4 |
| | 3 | 2.3043 | 4.891 |
| | 4 | 2.4776 | 4.65838 |
| 0.01 | 2 | 20.2018 | 4 |
| | 3 | 34.2724 | 2.07328 |
| | 4 | 21.6339 | 4.90848 |

and $\lambda = 628$ nm. Figure 4 shows the resolution as a function of α . A minimum indicated the best possible resolution. We can see that the four-photon setup performs worse than $N = 2$ and $N = 3$ in most regimes. In Table II, the resolution $\delta\theta$ is shown for the case where the ground-based photons are partially distinguishable from each other. The case of practical interest is how $N = 3$ compares to $N = 2$. For low occupancy $\varepsilon = 0.01$, the case $N = 2$ is already optimal. Figure 5 shows the resolution as a function of α .

We can further compare the performance of our protocol to a semiclassical protocol where s_2, \dots, s_N are replaced with a coherent state that is distributed between A and B (for example, by sending a coherent state $|\alpha\rangle$ into a beam splitter, and sending the two outputs to A and B), and photon counting at the receivers. In the lossless asymptotic limit with $\varepsilon = 1$ (the best-case scenario), this leads to a precision of $\Delta\theta = 2\sqrt{2}/kL$, which is worse than the achievable resolution

TABLE II. The table presents the parameters for $N = 3$ with varying degrees of distinguishability, using the identical $N = 2$ as reference. The enhancement in resolution is observed with $N = 3$; $\mathcal{S} = 96\%$ for each case corresponds to a distinct emission rate. This advantage disappears as distinguishability increases even with an additional photon at the ground base. As a result, boosting photon counts in practice does not necessarily guarantee improved estimation.

| ε | $N; \mathcal{S}\%$ | $\delta\theta_{\min}$ (μas) | α_{opt} |
|---------------|--------------------|--|-----------------------|
| 0.99 | 2; 100 | 2.030 | 4 |
| | 3; 96 | 1.468 | 4.192 |
| | 3; 50 | 2.033 | 4.098 |
| 0.5 | 3; 25 | 2.830 | 4.050 |
| | 2; 100 | 3.999 | 4 |
| | 3; 96 | 2.3030 | 4.8911 |
| 0.01 | 3; 50 | 3.1456 | 4.7868 |
| | 3; 25 | 4.2040 | 4.4409 |
| | 2; 100 | 19.980 | 4 |
| 0.01 | 3; 96 | 34.272 | 2.0732 |
| | 3; 50 | 43.449 | 2.0621 |
| | 3; 25 | 57.230 | 2.1542 |

shown in our Figs. 4 and 5. This coherent-state protocol is semiclassical because it depends on photon counting. We have not included this in the figures above, since the comparison is not quite so straightforward. In particular, we need to decide whether we allow for a very bright coherent state, which will require detectors that can tell the difference between n and $n + 1$ photons, where $n \gg 1$. These detectors do not exist (as opposed to single-photon sources and low-photon-number resolution detectors). Alternatively, we can choose the average photon number in the coherent state equal to the number of auxiliary photons. In this case, the precision will be much worse than the already inferior ideal case above.

We could further reduce the quantum mechanical nature from the protocol by considering homodyne detection. However, as was pointed out by Wang and Zhou in a recent paper

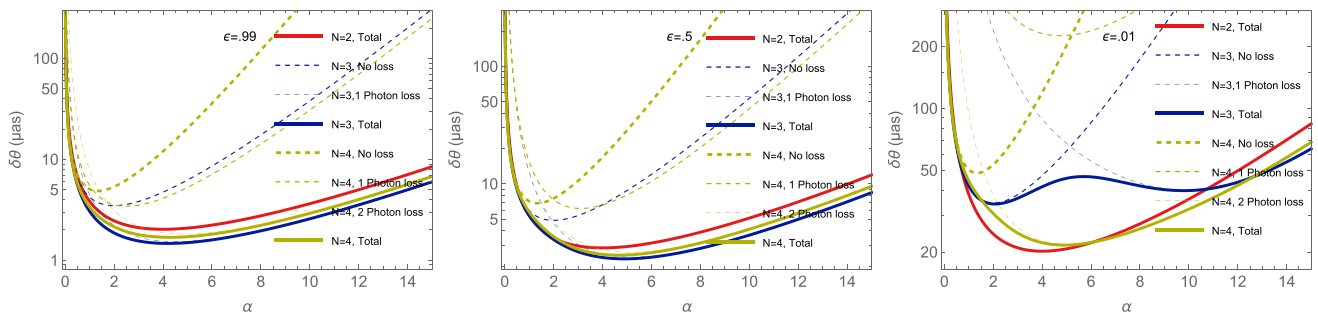


FIG. 4. The resolution angle $\delta\theta$ as a function of baseline length α in units of attenuation length $L_0 = 10$ km. The curves are obtained using the same optical wavelength as in Fig. 3 (628 nm) and different arrival probabilities of the star photon. The ground-based photons are considered to be nearly identical (96% indistinguishability) to the star photon. The panels from left to right indicate a decline in the rate of the arriving star photon. Different solid colors shown in each figure correspond to a different total photon number. The resolution for the first two figures appears to improve as the number of ground-based photons increases up to $N = 3$. However, because of complex interferences, increasing the number above $N = 3$ does not boost the resolution anymore. The improvement is reported to be broken even beyond $N = 2$ when the arrival rate of the star photon becomes highly uncertain, as shown in the panel to the right. Unlike the ideal case in Fig. 3, nearly identical ground-based photons do not always ensure lowering the minimum of resolution even when the arrival of the star photon is slightly uncertain. However, until $N = 3$ (Table I), the improvement is robust up to a moderate arrival rate of the star photon.

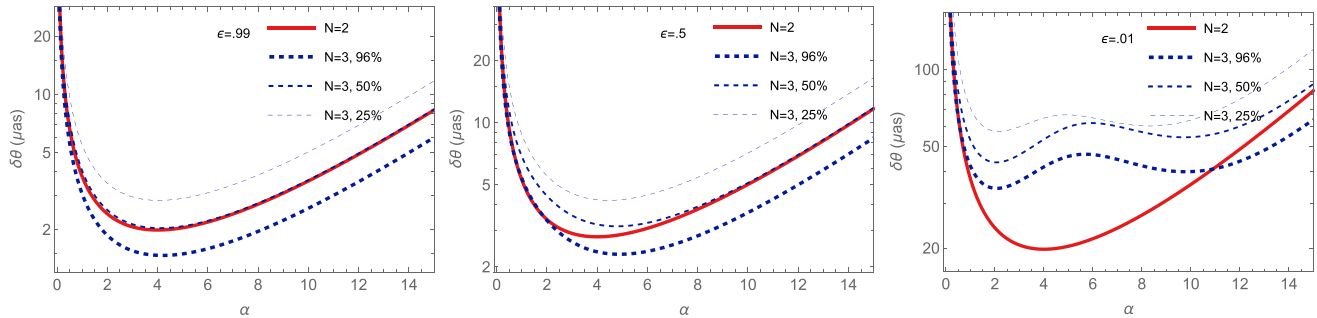


FIG. 5. The resolution angle $\delta\theta$ as a function of α for the same parametrization as in Fig. 4. The curves are also obtained for optical wavelengths $\lambda = 628$ nm, with the same attenuation length scale $L_0 = 10$ km. The panels, from left to right, indicate different arrival probabilities of the star photon. Each panel uses the solid red curve as a reference where the ground-based photon is indistinguishable from the stellar photon. The blue curves denote different levels of mutually distinguishable ground-based photons. The panel on the left shows that having more photons at the ground improves resolution, even if they can be distinguished to some extent. Once distinguishability reaches a particular threshold, the advantage is no longer available. The panel in the middle, when the arrival rate is much more uncertain than before, appears to follow the same pattern, but with a compromised resolution. Finally, if we take into account the situation where the rate of arrival is very uncertain, employing more ground-based photons is an unnecessary investment. We rule out the case with $N = 4$ since it appears to be an unsuitable option due to complex interference.

[21], such an all-Gaussian protocol will do still worse than the protocols presented here, since the Fisher information will be bounded by ε^2 , whereas our protocol scales with ε .

V. CONCLUSIONS

We considered the enhanced baseline two-receiver telescope, where quantum entanglement in the form of mode-entangled single photons are employed to help increase the baseline in the presence of loss. The astronomical photons carry the information about the object of interest, and minimizing their loss dictates that we measure them soon after they enter the telescope. The photons created on the ground do not carry information about the astronomical object, and we can therefore afford to lose some of them. Building redundancy by sending multiple photons to the receivers allows us to push the baseline much further, and as long as there is an appreciable photon flux in the detectors at the two receivers, we can increase the practical resolution of the telescope. We measure the resolution using the mean square error on the angular position in the sky, and we calculate the classical Fisher information to find the resolution limit via the classical Cramér-Rao bound.

In this paper we considered two open questions, namely, the effect of partial distinguishability of the photons and the effect of low occupancy of thermal modes. When the occupancy $\varepsilon = 1$, the resolution is relatively robust against moderate photon distinguishability, and four nearly identical photons (96% indistinguishability) strongly outperform the simple $N = 2$ case for a resolution of $\delta\theta = 1.23$ μs . However, even for a small reduction in $\varepsilon = 0.99$ and a distinguishability of 96%, the four-photon setup is outperformed by the three-photon case. Hence, we conclude that in practice we do not need to consider more than three photons, including the astronomical photon. For an occupancy of $\varepsilon = 0.5$ and indistinguishability of 96%, the three-photon case just outperforms the simplest case of $N = 2$. However, the situation changes considerably when the occupancy is reduced further. At $\varepsilon = 0.01$, increased distinguishability of the photons has

a pronounced detrimental effect on the $N = 3$ case, but the leading cause of lower resolution is the reduced occupancy of the astronomical mode.

For thermal states with a large ε (such as for lower-frequency radiation), our proposal also applies in principle. However, the analysis will be greatly complicated by the presence of multiple photons in the thermal modes, and in practice the calculations will become intractable very quickly, even using the relatively simple balanced beam-splitter setup in our interferometers U (the discrete QFTs). We expect to gain more information about the position of the source in the sky due to the additional photons, but this will be offset by the greater uncertainty about the number of photons that originate from the external source.

Another interesting effect is the contributions to the resolution of different numbers of measured photons in the $N = 3$ case. There are two contributions to the resolution, namely, when all photons are detected and when only two out of three photons are detected. These two contributions have very different optimal baseline scales, and the resolution curve has two minima, shown in Fig. 4. As a result, for thermal light sources in the near infrared or optical frequency domain, the optimal setup is also the simplest setup, with one auxiliary photon that is filtered to be indistinguishable to the astronomical photon to within a few percent. Yet, even in this setup resolutions on the order of ~ 20 μs should be achievable.

ACKNOWLEDGMENTS

This research was funded by the Engineering and Physical Sciences Research Council through the grants Large Baseline Quantum-Enhanced Imaging Networks (Grant No. EP/V021303/1) and Mathematical Tools for Practical Quantum Imaging Protocols (Grant No. UKRI069).

DATA AVAILABILITY

The data supporting this study's findings are available within the article.

APPENDIX: MODIFIED FISHER INFORMATION

We derive an expression for the modified Fisher information using two ground-based photons when a star emits photons at a rate ε substantially lower than 1. The density operator for the initial state of the starlight is approximated as described in Sec. IV. We write the total input state with two possibilities, i.e., one in the absence (A) and the other in the presence (B) of a star photon:

$$\begin{aligned} |\psi\rangle_A &= |0\rangle_1 \otimes |1\rangle_2 \otimes |1\rangle_3, \\ |\psi\rangle_B &= |1\rangle_1 \otimes |1\rangle_2 \otimes |1\rangle_3. \end{aligned} \quad (\text{A1})$$

Now, let the photons enter the interferometer and collect the state at the output:

$$\begin{aligned} |1\rangle_1 &\rightarrow \frac{1}{\sqrt{2}} \left(\frac{(e^{\frac{2i\pi}{3}} a_1^\dagger + e^{-\frac{2i\pi}{3}} a_2^\dagger + a_3^\dagger)}{\sqrt{3}} + \frac{e^{i\phi}(e^{\frac{2i\pi}{3}} b_1^\dagger + e^{-\frac{2i\pi}{3}} b_2^\dagger + b_3^\dagger)}{\sqrt{3}} \right)_1, \\ |1\rangle_2 &\rightarrow \frac{1}{\sqrt{2}} \left(\frac{\sqrt{1-p}(e^{-\frac{2i\pi}{3}} a_1^\dagger + e^{\frac{2i\pi}{3}} a_2^\dagger + a_3^\dagger)}{\sqrt{3}} + \sqrt{p}c_2^\dagger + \frac{\sqrt{1-p}(e^{-\frac{2i\pi}{3}} b_1^\dagger + e^{\frac{2i\pi}{3}} b_2^\dagger + b_3^\dagger)}{\sqrt{3}} + \sqrt{p}d_2^\dagger \right)_2, \\ |1\rangle_3 &\rightarrow \frac{1}{\sqrt{2}} \left(\frac{\sqrt{1-p}(a_1^\dagger + a_2^\dagger + a_3^\dagger)}{\sqrt{3}} + \sqrt{p}c_3^\dagger + \frac{\sqrt{1-p}(b_1^\dagger + b_2^\dagger + b_3^\dagger)}{\sqrt{3}} + \sqrt{p}d_3^\dagger \right)_3. \end{aligned} \quad (\text{A2})$$

We have treated all photons as identical and recorded every event associated with a single-photon loss. The contributions to Eq. (20) are as follows:

$$\begin{aligned} \mathcal{F}_2^1 &= \frac{\varepsilon^2 p^2 (1-p)^2 \sin^2 \phi}{3[\varepsilon p(1-p)(1+\cos \phi) + 4(1-\varepsilon)(1-p)^2]}, \\ \mathcal{F}_2^2 &= \frac{\varepsilon^2 p^2 (1-p)^2 (\sin \phi + \sqrt{3} \cos \phi)^2}{3[2\varepsilon p(1-p)[2 + \sqrt{3} \sin(\phi) - \cos(\phi)] + 4(1-\varepsilon)(1-p)^2]}, \\ \mathcal{F}_2^3 &= \frac{\varepsilon^2 p^2 (1-p)^2 (\sin \phi - \sqrt{3} \cos \phi)^2}{3[2\varepsilon p(1-p)(2 - \sqrt{3} \sin \phi - \cos \phi) + 4(1-\varepsilon)(1-p)^2]}. \end{aligned} \quad (\text{A3})$$

The situation where each ground-based photon has a distinct distinguishability from the reference photon is now examined. This will modify the contributions:

$$\begin{aligned} \mathcal{F}_2^1 &= \frac{\alpha_2^4 \beta_3^4 \varepsilon^2 p^2 (1-p)^2 \sin^2 \phi}{6[\varepsilon p(1-p) \alpha_2^2 \beta_3^2 (1+\cos \phi) + 4(1-\varepsilon)(1-p)^2 \alpha_2^2 \alpha_3^2]}, \\ \mathcal{F}_2^2 &= \frac{\alpha_3^4 \beta_2^4 \varepsilon^2 p^2 (1-p)^2 \sin^2 \phi}{6[\alpha_3^2 \beta_2^2 \varepsilon p(1-p)(1+\cos \phi) + 4\alpha_2^2 \alpha_3^2 (1-p)^2 (1-\varepsilon)]}, \\ \mathcal{F}_2^3 &= \frac{\alpha_3^4 \alpha_2^4 \varepsilon^2 p^2 (1-p)^2 \sin^2 \phi}{3[4\alpha_2^2 \alpha_3^2 (1-p)^2 (1-\varepsilon) + \alpha_2^2 \alpha_3^2 \varepsilon p(1-p)(1+\cos \phi)]}, \\ \mathcal{F}_2^4 &= \frac{\alpha_2^4 \beta_3^4 \varepsilon^2 p^2 (1-p)^2 (\sin \phi - \sqrt{3} \cos \phi)^2}{6[2\alpha_2^2 \beta_3^2 \varepsilon p(1-p)(2 - \sqrt{3} \sin \phi - \cos \phi) + 4\alpha_2^2 \alpha_3^2 (1-p)^2 (1-\varepsilon)]}, \\ \mathcal{F}_2^5 &= \frac{\alpha_3^4 \beta_2^4 \varepsilon^2 p^2 (1-p)^2 (\sin \phi + \sqrt{3} \cos \phi)^2}{6[2\alpha_3^2 \beta_2^2 p(1-p)\varepsilon(2 + \sqrt{3} \sin \phi - \cos \phi) + 4\alpha_2^2 \alpha_3^2 (1-p)^2 (1-\varepsilon)]}, \\ \mathcal{F}_2^6 &= \frac{\alpha_2^4 \alpha_3^4 \varepsilon^2 p^2 (1-p)^2 (\sin \phi - \sqrt{3} \cos \phi)^2}{3[4\alpha_2^2 \alpha_3^2 (1-p)^2 (1-\varepsilon) + 2\alpha_2^2 \alpha_3^2 p(1-p)\varepsilon(2 - \sqrt{3} \sin \phi - \cos \phi)]}, \\ \mathcal{F}_2^7 &= \frac{\alpha_3^4 \alpha_2^4 \varepsilon^2 p^2 (1-p)^2 [\sin(\phi) + \sqrt{3} \cos(\phi)]^2}{3[4\alpha_2^2 \alpha_3^2 (1-p)^2 (1-\varepsilon) + 2\alpha_2^2 \alpha_3^2 p(1-p)\varepsilon(2 + \sqrt{3} \sin \phi - \cos \phi)]}, \\ \mathcal{F}_2^8 &= \frac{\alpha_2^4 \beta_3^4 \varepsilon^2 p^2 (1-p)^2 (\sin \phi + \sqrt{3} \cos \phi)^2}{6[2\alpha_2^2 \beta_3^2 p(1-p)\varepsilon(2 + \sqrt{3} \sin \phi - \cos \phi) + 4\alpha_2^2 \alpha_3^2 (1-p)^2 (1-\varepsilon)]}, \\ \mathcal{F}_2^9 &= \frac{\alpha_3^4 \beta_2^4 \varepsilon^2 p^2 (1-p)^2 [\sin \phi - \sqrt{3} \cos(\phi)]^2}{6[2\alpha_3^2 \beta_2^2 p(1-p)\varepsilon(2 - \sqrt{3} \sin \phi - \cos \phi) + 4\alpha_2^2 \alpha_3^2 (1-p)^2 (1-\varepsilon)]}, \end{aligned} \quad (\text{A4})$$

where α_j is the degree of distinguishability between the reference and j th ground-based photon. It is clear that the contribution from the loss terms begins scaling up linearly as ε is approaching 1. On the other hand, when ε is significantly lower than 1, this refers to a situation where the rate of gaining information is reduced. Now, we carry out the same procedure using three ground-based photons. Unlike the earlier case, we have two sets of contributions: one for losing a single photon (\mathcal{F}_3^i) and other for losing two photons (\mathcal{F}_2^i). To keep things simple, we assume all the photons are identical, whereas the cases with distinguishability have been studied numerically. The following are the contributions to Eq. (21) for a single-photon loss:

$$\begin{aligned}
\mathcal{F}_3^1 &= \frac{\varepsilon^2 p^2 (1-p)^4 \cos^2 \phi}{4[2(1-\varepsilon)(1-p)^3 + \varepsilon p(1-p)^2(1-\sin \phi)]}, \\
\mathcal{F}_3^2 &= \frac{\varepsilon^2 p^2 (1-p)^4 \cos^2 \phi}{4[2(1-\varepsilon)(1-p)^3 + \varepsilon p(1-p)^2(1+\sin \phi)]}, \\
\mathcal{F}_3^3 &= \frac{6\varepsilon^2 p^2 (1-p)^4 \sin^2(\phi)}{4[18(1-\varepsilon)(1-p)^3 + \varepsilon p(1-p)^2(5+4\cos \phi)]}, \\
\mathcal{F}_3^4 &= \frac{\varepsilon^2 p^2 (1-p)^4 \sin^2 \phi}{2[2(1-\varepsilon)(1-p)^3 + \varepsilon p(1-p)^2(5-4\cos \phi)]}, \\
\mathcal{F}_3^5 &= \frac{\varepsilon^2 p^2 (1-p)^4 (\sin \phi + \cos \phi)^2}{2[4(1-\varepsilon)(1-p)^3 + 2\varepsilon p(1-p)^2(3+2\sin \phi - 2\cos \phi)]}, \\
\mathcal{F}_3^6 &= \frac{\varepsilon^2 p^2 (1-p)^4 (\sin \phi - \cos \phi)^2}{2[4(1-\varepsilon)(1-p)^3 + 2\varepsilon p(1-p)^2(3-2\sin \phi - 2\cos \phi)]}.
\end{aligned} \tag{A5}$$

Similarly, the contributions are as follows when two photons are lost:

$$\begin{aligned}
\mathcal{F}_2^1 &= \frac{p^4(1-p)^2 \varepsilon^2 \sin^2 \phi}{8[p^2(1-p)\varepsilon(1+\cos \phi) + 4p(1-p)^2(1-\varepsilon)]}, \\
\mathcal{F}_2^2 &= \frac{p^4(1-p)^2 \varepsilon^2 \sin^2 \phi}{16[p^2(1-p)\varepsilon(1-\cos \phi) + 2p(1-p)^2(1-\varepsilon)]}, \\
\mathcal{F}_2^3 &= \frac{p^4(1-p)^2 \varepsilon^2 \cos^2 \phi}{16[p^2(1-p)\varepsilon(1+\sin \phi) + 2p(1-p)^2(1-\varepsilon)]}, \\
\mathcal{F}_2^4 &= \frac{p^4(1-p)^2 \varepsilon^2 \sin^2 \phi}{16[p^2(1-p)\varepsilon(1-\cos \phi) + 2p(1-p)^2(1-\varepsilon)]}, \\
\mathcal{F}_2^5 &= \frac{p^4(1-p)^2 \varepsilon^2 \cos^2 \phi}{16[p^2(1-p)\varepsilon(1-\sin \phi) + 2p(1-p)^2(1-\varepsilon)]}, \\
\mathcal{F}_2^6 &= \frac{3p^4(1-p)^2 \varepsilon^2 \sin^2 \phi}{32[p^2(1-p)\varepsilon(1-\cos \phi) + 4p(1-p)^2(1-\varepsilon)]}, \\
\mathcal{F}_2^7 &= \frac{3p^4(1-p)^2 \varepsilon^2 \sin^2 \phi}{32[p^2(1-p)\varepsilon(1+\cos \phi) + 4p(1-p)^2(1-\varepsilon)]}, \\
\mathcal{F}_2^8 &= \frac{p^4(1-p)^2 \varepsilon^2 \sin^2 \phi}{8[p^2(1-p)\varepsilon(\cos \phi + 1) + 4p(1-p)^2(1-\varepsilon)]}, \\
\mathcal{F}_2^9 &= \frac{p^4(1-p)^2 \varepsilon^2 \sin^2 \phi}{16[p^2(1-p)\varepsilon(1-\cos \phi) + 2p(1-p)^2(1-\varepsilon)]}, \\
\mathcal{F}_2^{10} &= \frac{p^4(1-p)^2 \varepsilon^2 \cos^2 \phi}{16[p^2(1-p)\varepsilon(\sin \phi + 1) + 2p(1-p)^2(1-\varepsilon)]}, \\
\mathcal{F}_2^{11} &= \frac{p^4(1-p)^2 \varepsilon^2 \sin^2 \phi}{16[p^2(1-p)\varepsilon(1-\cos \phi) + 2p(1-p)^2(1-\varepsilon)]}, \\
\mathcal{F}_2^{12} &= \frac{p^4(1-p)^2 \varepsilon^2 \cos^2 \phi}{16[p^2(1-p)\varepsilon(1-\sin \phi) + 2p(1-p)^2(1-\varepsilon)]}, \\
\mathcal{F}_2^{13} &= \frac{p^4(1-p)^2 \varepsilon^2 \sin^2 \phi}{32[p^2(1-p)\varepsilon(\cos \phi + 1) + 4p(1-p)^2(1-\varepsilon)]},
\end{aligned}$$

$$\mathcal{F}_2^{14} = \frac{p^4(1-p)^2\varepsilon^2 \sin^2 \phi}{32[p^2(1-p)\varepsilon(1-\cos \phi) + 4p(1-p)^2(1-\varepsilon)]},$$

$$\mathcal{F}_2^{15} = \frac{1}{2}(1-p)p^2\varepsilon, \quad (\text{A6})$$

with $\varepsilon \rightarrow 1$, and both the sets corresponding to the loss start scaling up linearly, whereas for small ε , the error in estimation becomes more dominant.

-
- [1] D. Dravins, Intensity interferometry: Optical imaging with kilometer baselines, *Proc. SPIE* **9907** 99070(M) (2016).
- [2] R. Czupryniak, J. Steinmetz, P. G. Kwiat, and A. N. Jordan, Optimal qubit circuits for quantum-enhanced telescopes, *Phys. Rev. A* **108**, 052408 (2023).
- [3] M. R. Brown, M. Allgaier, V. Thiel, J. D. Monnier, M. G. Raymer, and B. J. Smith, Interferometric imaging using shared quantum entanglement, *Phys. Rev. Lett.* **131**, 210801 (2023).
- [4] M. Bojer, Z. Huang, S. Karl, S. Richter, P. Kok, and J. von Zanthier, A quantitative comparison of amplitude versus intensity interferometry for astronomy, *New J. Phys.* **24**, 043026 (2022).
- [5] K. Akiyama, A. Alberdi, W. Alef, K. Asada, R. Azulay, A.-K. Bacsko, D. Ball, M. Baloković, J. Barrett, D. Bintley *et al.*, First M87 event horizon telescope results. IV. Imaging the central supermassive black hole, *Astrophys. J. Lett.* **875**, L4 (2019).
- [6] M. I. Kolobov, *Quantum Imaging* (Springer Science & Business Media, New York, 2007).
- [7] M. Tsang, R. Nair, and X.-M. Lu, Quantum theory of superresolution for two incoherent optical point sources, *Phys. Rev. X* **6**, 031033 (2016).
- [8] M. Tsang, Resolving starlight: a quantum perspective, *Contemp. Phys.* **60**, 279 (2019).
- [9] M. E. Pearce, E. T. Campbell, and P. Kok, Optimal quantum metrology of distant black bodies, *Quantum* **1**, 21 (2017).
- [10] L. A. Howard, G. G. Gillett, M. E. Pearce, R. A. Abrahao, T. J. Weinhold, P. Kok, and A. G. White, Optimal imaging of remote bodies using quantum detectors, *Phys. Rev. Lett.* **123**, 143604 (2019).
- [11] C. Lupo, Z. Huang, and P. Kok, Quantum limits to incoherent imaging are achieved by linear interferometry, *Phys. Rev. Lett.* **124**, 080503 (2020).
- [12] U. Zanforlin, C. Lupo, P. W. Connolly, P. Kok, G. S. Buller, and Z. Huang, Optical quantum super-resolution imaging and hypothesis testing, *Nat. Commun.* **13**, 5373 (2022).
- [13] D. Gottesman, T. Jennewein, and S. Croke, Longer-baseline telescopes using quantum repeaters, *Phys. Rev. Lett.* **109**, 070503 (2012).
- [14] Z. Huang, G. K. Brennen, and Y. Ouyang, Imaging stars with quantum error correction, *Phys. Rev. Lett.* **129**, 210502 (2022).
- [15] M. M. Marchese and P. Kok, Large baseline optical imaging assisted by single photons and linear quantum optics, *Phys. Rev. Lett.* **130**, 160801 (2023).
- [16] L. Hardy, Nonlocality of a single photon revisited, *Phys. Rev. Lett.* **73**, 2279 (1994).
- [17] A. Peres, Nonlocal effects in Fock space, *Phys. Rev. Lett.* **74**, 4571 (1995).
- [18] L. Vaidman, Nonlocality of a single photon revisited again, *Phys. Rev. Lett.* **75**, 2063 (1995).
- [19] L. Hardy, Hardy replies, *Phys. Rev. Lett.* **75**, 2065 (1995).
- [20] L. Mandel, *Optical Coherence and Quantum Optics* (Cambridge University, Cambridge, England, 1995).
- [21] Y. Wang and S. Zhou, Limitations of Gaussian measurements in quantum imaging, [arXiv:2503.06363](https://arxiv.org/abs/2503.06363).